

A Realtime Weather-Adaptive Hybrid ensemble 3DVAR Analysis System with Automatic Storm Positioning and On-demand Capability

Jidong Gao¹, Chenghao Fu^{1,2}, Darrel Kingfield^{1,2}, Kristin Calhoun^{1,2},
Chris Karstens^{1,2}, Travis Smith^{1,2}, Gerry Creager^{1,2}, Lou Wicker¹, and Jack Kain¹

¹NOAA/National Severe Storm Laboratory, Norman, OK 73072, and

²Cooperative Institute for Mesoscale Meteorological Studies,
University of Oklahoma, Norman, OK 73072

1. Introduction

The proper early identification of a supercell thunderstorm, or a supercell imbedded in a cluster of storms, is critical to the issuance of public warnings for severe weather, especially in a day when the environment is unstable and favorable to produce severe weather. Several studies by Burgess (1976), Burgess and Lemon (1991), and Bunkers et al. (2006, 2009) found the determination of whether or not a thunderstorm is a supercell thunderstorm is very important to accurate and timely severe weather warning operations. These studies revealed that many supercells produce tornadoes, large hail, or severe surface winds.

One of the most important indicators of a supercell is the existence of a mid-level mesocyclone. The mesocyclone is defined as the Doppler radar velocity signature of a storm-scale (2–10-km diameter) vortex (Burgess, 1976) which corresponds to the rotating updraft–downdraft couplet of a supercell thunderstorm. Mesocyclones in the United States are often cyclonic and may also contain the more intense tornado vortex. Most of time, when strong supercells develop, the embedded mesocyclone can be very deep and narrow (Gao et al. 2013). In the last twenty years, several criteria have been established for mesocyclone recognition based on a wealth of Doppler radar observations, especially after the implementation of WSR-88Ds (Burgess et al. 1982, 1991, 1993; Stumpf et al., 1998). However, sometimes it is still very difficult to identify mesocyclones from radars, especially when so many storm cells may exist in a large area such as the big tornado outbreak of April 27th, 2011 in the South Eastern United States.

In this situation, the workload and timeliness requirement may limit forecasters' ability to effectively use WSR-88Ds and other information to issue correct and timely warnings. The use of fast data assimilation methods, such as the 3DVAR, may provide a potential

solution for merging available information as quickly as possible for human decision makers. The 3DVAR program (Gao et al. 1999; 2002; 2004) developed for the Advanced Regional Prediction System (ARPS, Xue et al. 2000; 2001; 2003) has been used for such purpose in recent years. The system was implemented to provide detail convective scale three-dimension wind information which includes the derived products vertical vorticity and vertical velocity fields to NWS forecasters at the NOAA/Hazardous Weather Testbed (HWT) for several spring experiments (Gao et al. 2013). The National Centers for Environmental Prediction (NCEP) North American Mesoscale (NAM) model forecasts were used as a background field and data from several WSR-88Ds assimilated to provide a convective-scale three-dimensional storm analysis the HWT Experimental Warning Program. Forecasters using these analyses in warning-decision processes found the products had a high potential for warning operations (Smith et al. 2014; Calhoun et al. 2014).

In this study, we investigate the possibility of incorporating ensemble information into the 3DVAR system called a real-time, weather-adaptive hybrid three-dimensional ensemble variational data assimilation (3DEnVAR) system. The preliminary 3DEnVAR system was developed and tested for the idealized thunder storm case in Gao and Stensrud (2014), but it was coupled with an EnKF system. Stensrud and Gao (2010) suggested that knowledge of horizontal environmental variability is important to successful convective-scale analyses and predictions and should be used in realtime analysis and forecast system. As we know, NCEP short-range ensemble forecasting (SREF) may provide good information about mesoscale environmental variability. By using this information, the quality of the analysis may be improved, but the overall computational cost should not be significantly increased over the original 3DVAR system because no ensemble forecasts are needed. The system retains the fine features of the original 3DVAR system (Gao et al. 2013; Smith et al. 2014). For example, it has the ability to automatically detect and analyze severe local hazardous weather events and the analysis can also be performed with an on-demand capability where end-users (e.g., forecasters or

¹Corresponding author address: Dr. Jidong Gao,

NOAA/National Severe Storm Laboratory,
120 David Boren Blvd, Norman OK 73072.

Email: jidong.gao@noaa.gov.

scientists) identify the location of the analysis domain in real time based on the current weather situation.

Although still in the early development stage, the hybrid 3DnVAR the system was tested during the 2015 HWT spring experiments. Many severe weather events were automatically detected and analyzed.

Section 2 provides an overview of the data assimilation (DA) system. Three Selected Cases for 2015 spring experiments are reported in section 3. We conclude in section 4 with a summary and outlook for future work.

2. The ARPS 3DVAR and Procedure Description

The original ARPS 3DVAR (Gao et al. 1999, 2002, 2004; Hu et al. 2006), designed especially for storm-scale data assimilation, uses a recursive filter (Purser et al. 2003) with a mass continuity equation and other constraints that are incorporated into a cost function, yielding physically-consistent three-dimensional analyses of the wind components and other model variables. Multiple analysis passes are used that have different spatial influence scales in order to accurately represent intermittent convective storms, while the quality control steps within the ARPS 3DVAR also are very important to improving the quality of the radial velocity and reflectivity data. A hybrid 3DnVAR DA system has been developed based on the existing ARPS 3DVAR system (Gao and Stensrud 2014). The algorithm uses the extended control variable approach to combine the static and ensemble-derived flow-dependent forecast error covariances (Lorenc 2003; Buehner 2005; Wang et al. 2007). The method was applied to the assimilation of radar data from a simulated supercell storm in Gao and Stensrud (2014). In this study, the ensemble information is provided by NCEP's SREF product, not an EnKF system.

A real-time weather-dependent hazardous weather analysis and detection system based upon this 3DVAR method is developed to identify supercells and other severe weather events using data mainly from the WSR-88D network, and from the NCEP NAM 12 km resolution analyses and forecasts (Gao et al. 2013). The steps needed to make such a system operationally in real time are as follows (Fig. 1).

First, we obtain the two-dimensional composite reflectivity product from the National Severe Storm Laboratory (NSSL) MRMS system once per hour, and use it to identify a potential location (longitude, latitude) at greatest risk for severe storms. The identified location is used as the centers for the 3DVAR analysis domain. Parameters are then selected for the analysis domain, including the number of grid points, n_x , n_y , and n_z in the three spatial directions and the grid spac-

ings dx , dy , and dz . For the current study, we chose $n_x=n_y=240$, $dx=dy=1.5$ km. In the vertical, we use 31 terrain-following vertical layers, with nonlinear stretching, via a hyperbolic tangent function, yielding an average vertical grid spacing of 400 m. Once the domain is defined, the terrain data are interpolated to the analysis grids. The challenge here is to select a domain that is large enough to contain the principal features of meteorological interest while maintaining an efficient computational advantage so that the analyses can be produced fast enough to be of use in operations. Currently, the domain size is 360kmX360km. This will be enlarged in the future when the computational power is increased.

The second step, once the analysis domain is selected, is to obtain the necessary ensemble background fields. For this, we use the NCEP operational SREF analysis and forecast ensemble product, and interpolate it to the analysis domain in both space and time using existing software developed within the ARPS model. Third, we determine how many operational WSR-88Ds are present within the selected domain. To make assure the maximum data coverage, a large domain (560km X 560km) is used, and the the available WSR-88D data within that domain are obtained in real-time. Then, a necessary quality control is performed on these radar observations. After this, thinning, and interpolation of the radar data onto the analysis grids are performed.

The fourth step is to conduct the 3DnVAR analysis using both the background field obtained from step two, and the WSR-88D data obtained from step 3. Any additional available real-time data, such as mesonet data can be also used within this analysis with little additional computational cost.

The final step is the post processing of the resulting analyses, including identifying the position of supercells, obtaining two-dimensional composite vorticity tracks and two dimensional vertical velocity tracks from analysis, and producing other products that can be effectively used by the forecasters who issue severe weather warnings. This 5-step procedure is performed every 5 minutes or longer depending on computational cost and users' needs. Currently, by carefully choosing the domain size and number of vertical levels, in relation to our available computer (SGI Altix, 128 cores, Message Passing Interface [MPI]) capacity, each analysis can be finished within 5 minutes. By using all available information simultaneously, it is possible to determine the 3D winds and other variables as accurately as possible, while also improving the quality of reflectivity data coverage. As an initial application, in the analyses that follow, we only focus on the 3D wind analyses and wind-derived variables, especially vertical vorticity.

3. Three Selected Cases for 2015 spring experiments

The above system was implemented during the 2015 spring experiments for informal display purposes. We present here the performance of the system by examining three example severe weather cases observed during the 2015 spring experiments. We followed the procedure described in the last section. The analysis domain is floated based on MRMS 2D composite reflectivity product.

The first case is a tornadic supercell event that took place on 12 April 2015 near Garden City, South-West corner of Kansas. One supercell developed and produced hail and one tornado touched down according to SPC storm reports (Fig 2a). The analyses were performed using data from 8 nearby WSR-88Ds (Fig. 2b). In this first example, the evolution of the supercell storm during one hour, from 0000 UTC – 0100 UTC April 12, are shown in Figure 3, and are indicated by the horizontal winds (vectors), and vertical vorticity (black contours) and analyzed radar reflectivity (color shaded) at the 3 km height above ground. During this one hour period, it was very obvious that the storm developed from a weak echo single ordinal cell to a strong hook-echo related supercell in the reflectivity field. The vertical vorticity in 3DVAR analysis was also very weak at the beginning of the analysis (Fig. 3a). Gradually, the rotation became stronger, reached 0.012 s^{-1} after half an hour and maintained this level for about one hour (Fig. 3d, not fully shown). In reality, a tornado touched down during this period. It was found in the analysis that this very strong mid-level circulation (black contours) persisted and was co-located with reflectivity hook echo until the end of the analysis. This cell moved very slowly from west to east during the analysis period. The mesocyclone maintained its strength and vertical extent of 10 km depth (not shown) through the analysis period. During this period, the storm also produced large hail according to SPC reports (Fig 2a).

The second case includes multi-tornado events that took place in North Texas, in an area bounded by the Oklahoma-Texas border, and west of the city of Dallas (Figs. 4a). For this case, reflectivity and radial velocity observations from eight nearby WSR-88Ds were used in the 3DVAR analysis (Fig 4b). Over a 3.5 hour period (2100 UTC, 8 May – 0030 UTC, 9 May), 9 tornadoes touched down near the border of Oklahoma and Texas, in Wilbarger and Wichita counties of North Texas. Our automatic-domain analyses followed these events quite well. Fig. 5 shows one hour analyses from 2120 UTC to 2220 UTC. In the analyses, there were two very strong rotational centers (indicated by black contours, the maximum vorticity above 0.01 s^{-1} in Fig. 5c, d, e, f) associated with two strong mesocyclones throughout the analysis period. These moved slowly from west to east and the two reflectivity cores

demonstrated strong hook echoes. The North Texas supercell storm produced three tornadoes during this period. Another supercell near the Oklahoma-Texas border produced several tornadoes a hour later (Fig 4a).

The third case is a tornadic supercell storm which occurred in south Kansas (Fig 6a). For this case, observations from four WSR-88Ds were used, and no radar closely observed the supercell storms that produced two tornadoes (Fig. 6b). However, by utilizing all of the information from these multiple radars, the supercell which produced two tornadoes was easily identified from the analysis. Fig. 7 shows the series of the analyses during the period from 0300 UTC to 0350 UTC, 4 June. There were several ordinary storm cells inside the analysis domain. It was hard to figure out which one may produce tornado initials (Fig. 7a). However, as time progressed, one storm cell in the domain became stronger, circulation strengthened, and produced two tornadoes were produced (Fig. 6a, 7). Monitoring the trend of these analyses may help the forecasters issue severe weather warnings as reported in Calhoun et al. (2014).

4. Summary

Radar is a fundamental tool for severe storm monitoring and nowcasting activities. Forecasters examine real-time WSR-88D observations, radar algorithm products, and use their considerable experience and situational awareness to issue severe storm warnings that help protect the public from hazardous weather events. However, there are situations for which even well-trained forecasters find it challenging to make a quick and sound judgment based on information from radar and other sources. To take advantage of the information content from both the WSR-88D network and NCEP high resolution operational model analysis and forecast products, we developed a weather-adaptive analysis system which can be used for severe weather detections, especially detection of mesocyclones at middle atmospheric levels from 3-8 kilometers. The method used is the extension of the 3DVAR method in which partial of the background error covariance is derived from NCEP SREF ensemble product. The system may have potential to provide improved information for making severe weather warning decisions. The analysis method can be run offline. This enables us to study specific area in greater detail or to investigate the evolution and lifecycle of certain kinds of severe weather.

The analysis product can be produced in near realtime (4-5 minutes delay) for the NWS forecasters as demonstrated as one of the projects of the NOAA's HWT since spring 2011. The potential of this method has been shown by detecting the initiation and evolution of supercells from many real data cases. In this

report, we only show three examples, from the 2015 HWT Spring experiment. While we recognize that this method is very useful for identifying tracks of supercell thunderstorms, analyses may provide more intuitive products that can be effectively used by forecasters. In addition, the output of a 3DVAR analysis can be used to initialize short term convective scale NWP for the Warn-on-Forecast project, which will comprise a major portion of our near future work.

Acknowledgments. This research was primarily funded by NOAA/Warning on Forecast project and by NSF grants AGS-1341878. Chenghao Fu was also partially supported by a research and development fund of Chinese Meteorological Administration for Public Welfare Industrial Meteorology grant GYHY201306016. The assistance of NSSL IT team, Brett Morrow and Steve Fletcher are gratefully acknowledged for their computational support.

REFERENCES

- Buehner, M., 2005: Ensemble-derived stationary and flow-dependent background-error covariances: evaluation in a quasi-operational NWP setting. *Quart. J. Roy. Meteor. Soc.*, **131**, 1013-1043.
- Bunkers, M. R. Hjelmfelt, and P. L. Smith, 2006: An observational examination of long-lived supercells. Part I: Characteristics, evolution, and demise. *Wea. Forecasting*, **21**, 673-688.
- Bunkers, M. R., D. R. Clabo, and J. W. Zeitler, 2009: Comments on "Structure and Formation Mechanism on the 24 May 2000 Supercell-Like Storm Developing in a Moist Environment over the Kanto Plain, Japan". *Mon. Wea. Rev.*, **137**, 2703-2711.
- Burgess, D. W., 1976: Single Doppler radar vortex recognition: Part I—Mesocyclone signatures. Preprints, 17th Conf. on Radar Meteorology, Seattle, WA, Amer. Meteor. Soc., 97-103.
- Burgess, D. W., V. T. Wood, and R. A. Brown, 1982: Mesocyclone evolution statistics. Preprints, 12th Conf. on Severe Local Storms, San Antonio, TX, Amer. Meteor. Soc., 422-424.
- Burgess, D. W., and L. R. Lemon, 1991: Characteristics of mesocyclones detected during a NEXRAD test. Preprints, 25th Int. Conf. on Radar Meteorology, Paris, France, Amer. Meteor. Soc., 39-42.
- Burgess, D.W., Doswell, C.A., 1993. Tornadoes and tornadic storms: a review of conceptual models. The Tornado: Its Structure, Dynamics, Prediction and Hazards. Geophys. Monogr., vol. 79. Amer. Geophys. Union, pp. 161-172.
- Calhoun, K., M., T. M. Smith, D. M. Kingfield, J. Gao, and D. J. Stensrud, 2014: Forecaster Use and Evaluation of realtime 3DVAR analyses during Severe Thunderstorm and Tornado Warning Operations in the Hazardous Weather Testbed. *Wea. Forecasting* **29**, 601-613.
- Gao, J., M. Xue, A. Shapiro, and K.K. Droegemeier, 1999: A variational method for the retrieval of three-dimensional wind fields from dual-Doppler radars. *Mon. Wea. Rev.*, **127**, 2128-2142.
- Gao, J., M. Xue, K. Brewster, F. Carr, and K. K. Droegemeier, 2002: New Development of a 3DVAR system for a nonhydrostatic NWP model. Preprint, *15th Conf. Num. Wea. Pred. and 19th Conf. Wea. Anal. Forecasting*, San Antonio, TX, Amer. Meteor. Soc., 339-341.
- Gao, J., M. Xue, K. Brewster, and K. K. Droegemeier 2004: A three-dimensional variational data assimilation method with recursive filter for single-Doppler radar, *J. Atmos. Oceanic. Technol.* **21**, 457-469.
- Gao, J., T. M. Smith, D. J. Stensrud, C. Fu, K. Calhoun, K. L. Manross, J. Brogden, V. Lakshmanan, Y. Wang, K. W. Thomas, K. Brewster, and M. Xue, 2013: A realtime weather-adaptive 3DVAR analysis system for severe weather detections and warnings with automatic storm positioning capability. *Wea. Forecasting*, **28**, 727-745.
- Gao, J. and D. J. Stensrud, 2014: Some Observing System Simulation Experiments with a Hybrid 3DVAR System for Stormscale Radar Data Assimilation, *Mon. Wea. Rev.*, **142**, 3326-3346.
- Hu, M., M. Xue, J. Gao and K. Brewster, 2006: 3DVAR and Cloud Analysis with WSR-88D Level-II Data for the Prediction of the Fort Worth, Texas, Tornadic Thunderstorms. Part II: Impact of Radial Velocity Analysis via 3DVAR. *Mon. Wea. Rev.*, **134**, 699-721.
- Lemon, L. R., and C. A. Doswell III, 1979: Severe thunderstorm evolution and mesocyclone structure as related to tornadogenesis. *Mon. Wea. Rev.*, **107**, 1184-1197.
- Lorenc, A., 2003: The potential of the ensemble Kalman filter for NWP - a comparison with 4DVar. *Quart. J. Roy. Meteor. Soc.*, **129**, 3183-3204.
- Purser, R. J., W.-S. Wu, D. Parrish, and N. M. Roberts, 2003: Numerical aspects of the application of recursive filters to variational statistical analysis. Part I: Spatially homogeneous and isotropic Gaussian covariances. *Mon. Wea. Rev.*, **131**, 1524-1535.
- Smith, T. M., J. Gao, K. M. Calhoun, D. J. Stensrud, K. L. Manross, K. L. Ortega, C. Fu, D. M. Kingfield, K. L. Elmore, V. Lakshmanan, and C. Riedel, 2014: Performance of a real-time 3DVAR analysis system in the Hazardous Weather Testbed. *Wea. Forecasting*, **29**, 63-77.

- Stensrud D. J. and J. Gao, 2010: Importance of horizontally inhomogeneous environmental initial conditions to ensemble storm-scale radar data assimilation and very short range forecasts. *Mon. Wea. Rev.*, **138**, 1250-1272.
- Stumpf, G. J., A. Witt, E. D. Mitchell, P. L. Spencer, J.T. Johnson, M. D. Eilts, K. W. Thomas, D. W. Burgess, 1998: The National Severe Storms Laboratory Mesocyclone Detection Algorithm for the WSR-88D. *Weather and Forecasting*, **13**, 304-326.
- Wang, X., C. Snyder, and T. M. Hamill, 2007: On the theoretical equivalence of differently proposed ensemble/3D-Var hybrid analysis schemes. *Mon. Wea. Rev.* **135**, 222-227.
- Xue, M., K. K. Droegemeier, and V. Wong, 2000: The Advanced Regional Prediction System (ARPS)—A multiscale nonhydrostatic atmospheric simulation and prediction model. Part I: Model dynamics and verification. *Meteor. Atmos. Phys.*, **75**, 161-193.
- Xue, M., and Coauthors, 2001: The Advanced Regional Prediction System (ARPS)—A multiscale nonhydrostatic atmospheric simulation and prediction tool. Part II: Model physics and applications. *Meteor. Atmos. Phys.*, **76**, 134-165.
- Xue, M., D. Wang, J. Gao, K. Brewster, and K. K. Droegemeier, 2003: The Advanced Regional Prediction System (ARPS), storm-scale numerical weather prediction and data assimilation. *Meteor. Atmos. Phys.*, **76**, 143-165.

Flow Chart of the weather-adaptive 3DVAR System

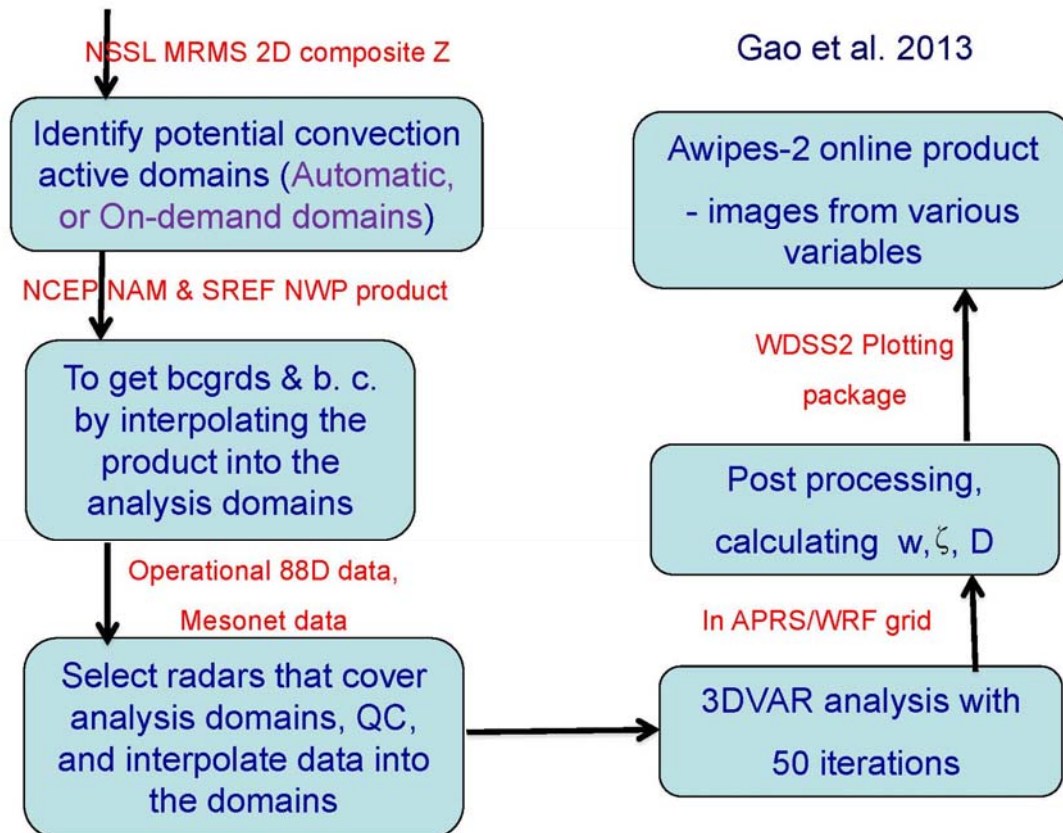


Fig. 1. Flow chart of realtime ensemble 3DVAR analysis.

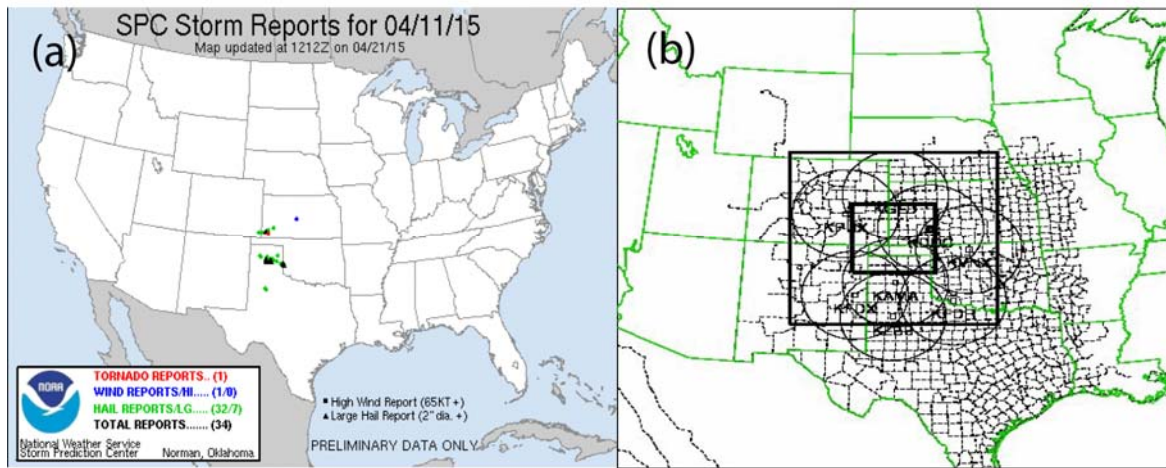


Fig. 2. April 12, 2015 Southwestern Kansas tornadic storm event. (a) The storm report from Storm Prediction Center (SPC); and (b) the illustration of 3DVAR analysis domain. The inner domain of 360x360 km is used for 3DVAR analysis. The outer domain of 560x560 km is used to identify WSR88D radars to be used.

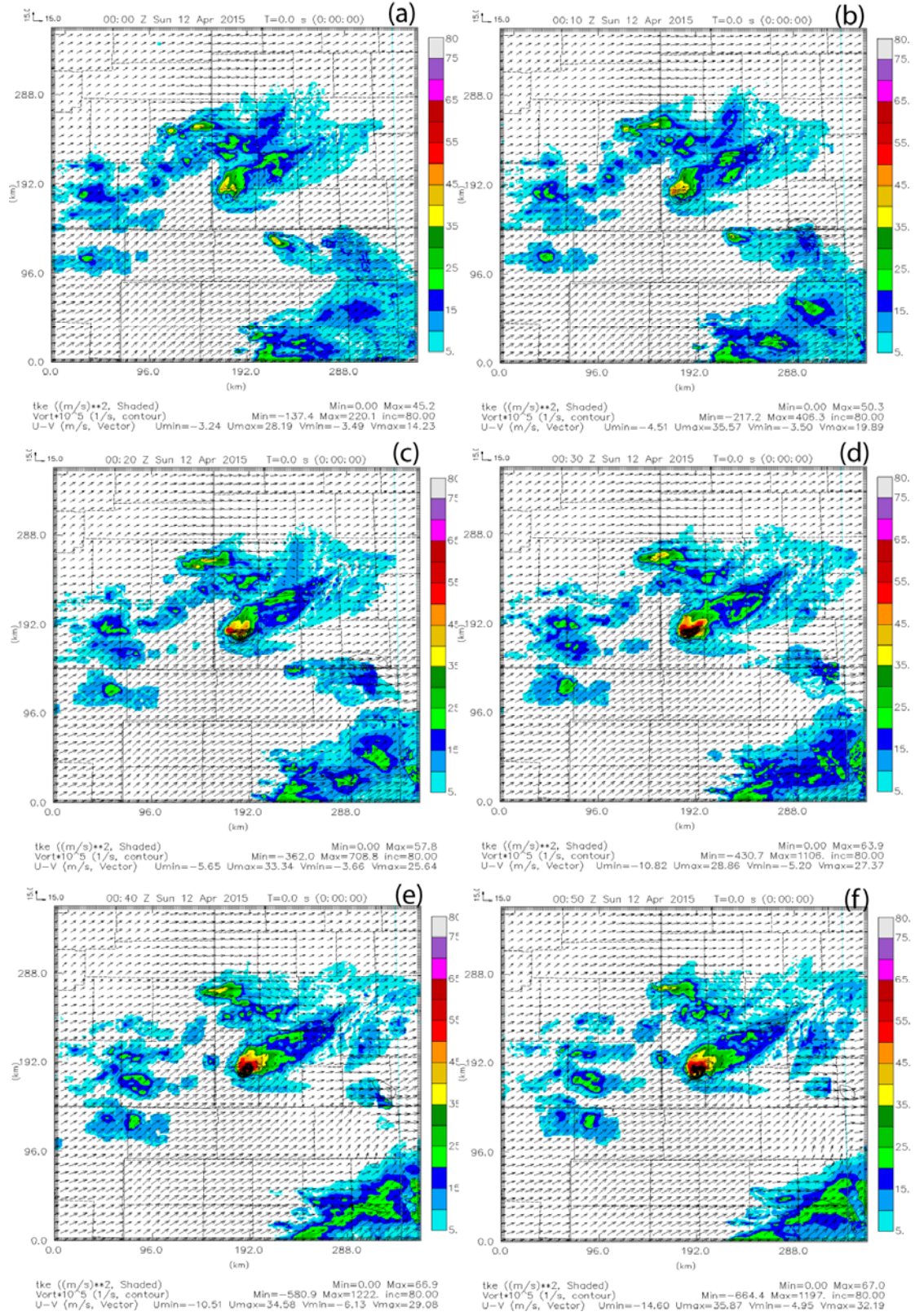


Fig. 3. The analyzed reflectivity, horizontal wind fields, and vorticity at $z=3$ km using data from radars displayed in Fig. 2(b) valid at (a) 0000 UTC, (b) 0010 UTC, (c) 0020 UTC, (d) 0030 UTC, (e) 0040 UTC, and (f) 0050 UTC, April 12, 2015 near southwestern KS.

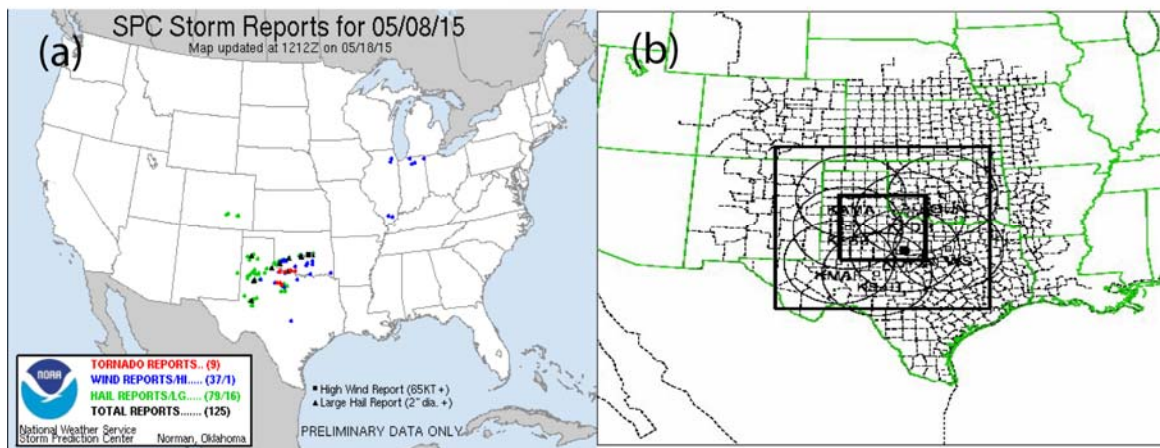


Fig. 4. Same as Fig. 2, but for tornadic storm events at Oklahoma Texas Border May 08, 2015.

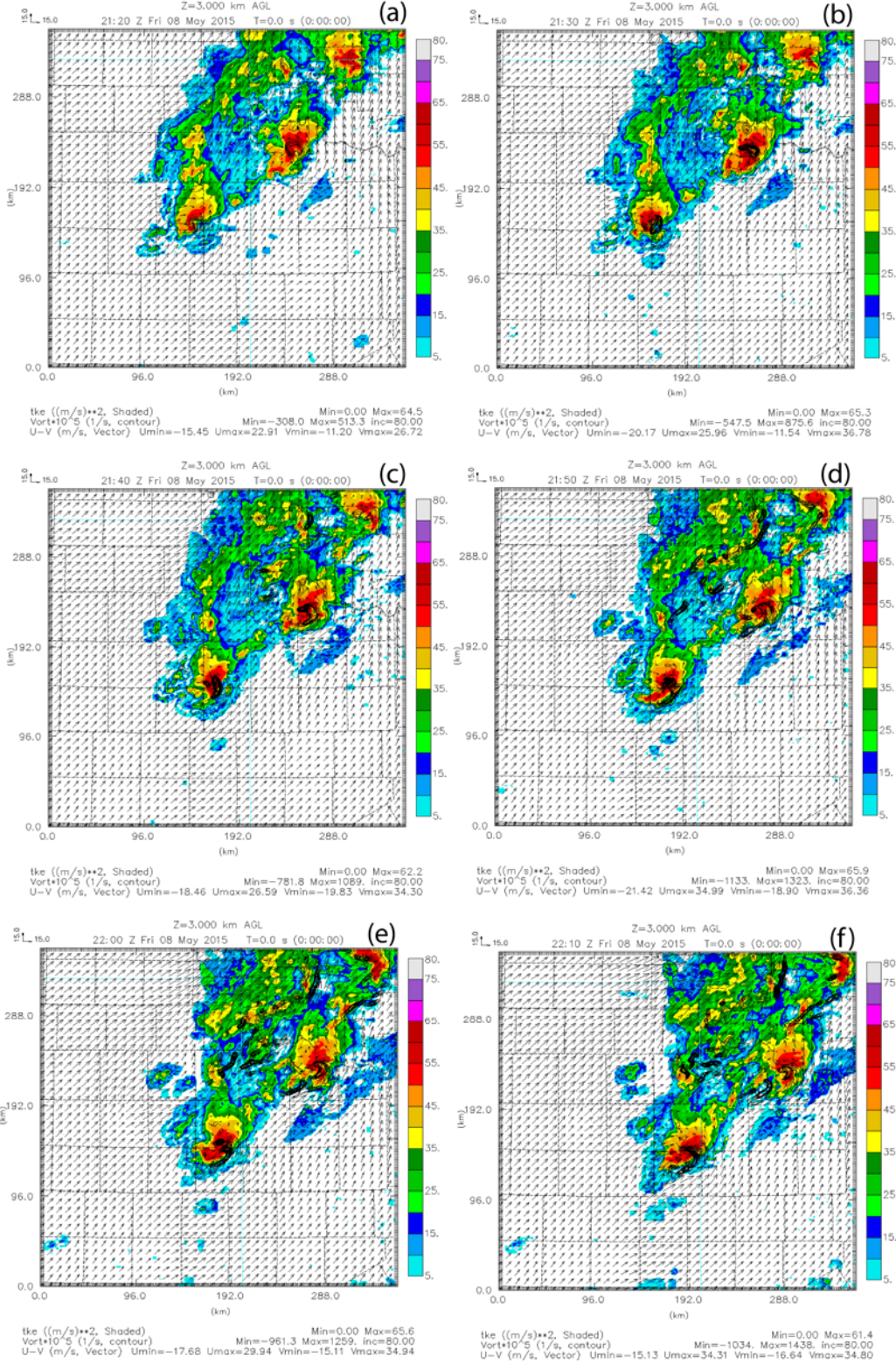


Fig. 5. The analyzed reflectivity, horizontal wind fields, and vortices at $z=3$ km using data from radars in Fig. 4(b) valid at (a) 2120 UTC, (b) 2130 UTC, (c) 2140 UTC, (d) 2150 UTC, (e) 2200 UTC, and (f) 2210 UTC, May 08, 2015 near the border of Oklahoma and Texas.

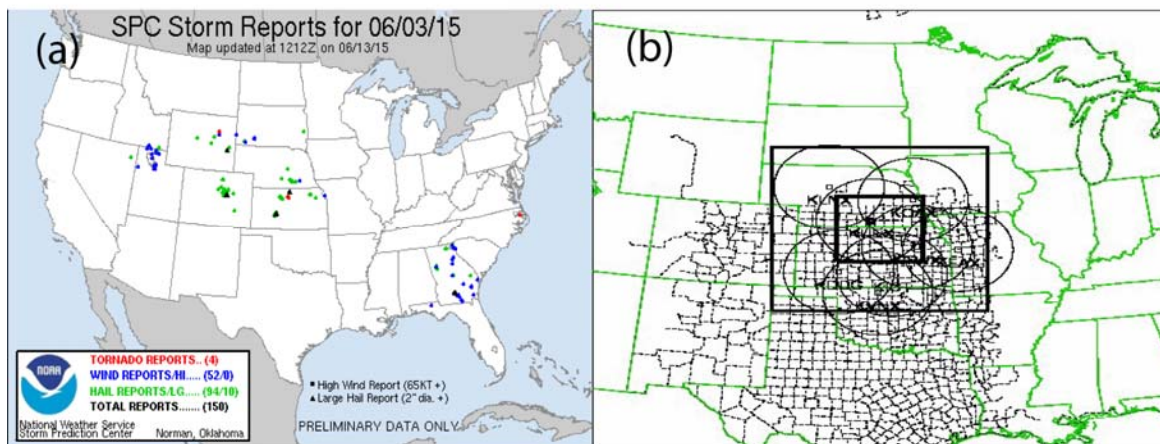


Fig. 6. Same as Fig. 2, but for south Kansas tornadic storm event on June 03, 2015.

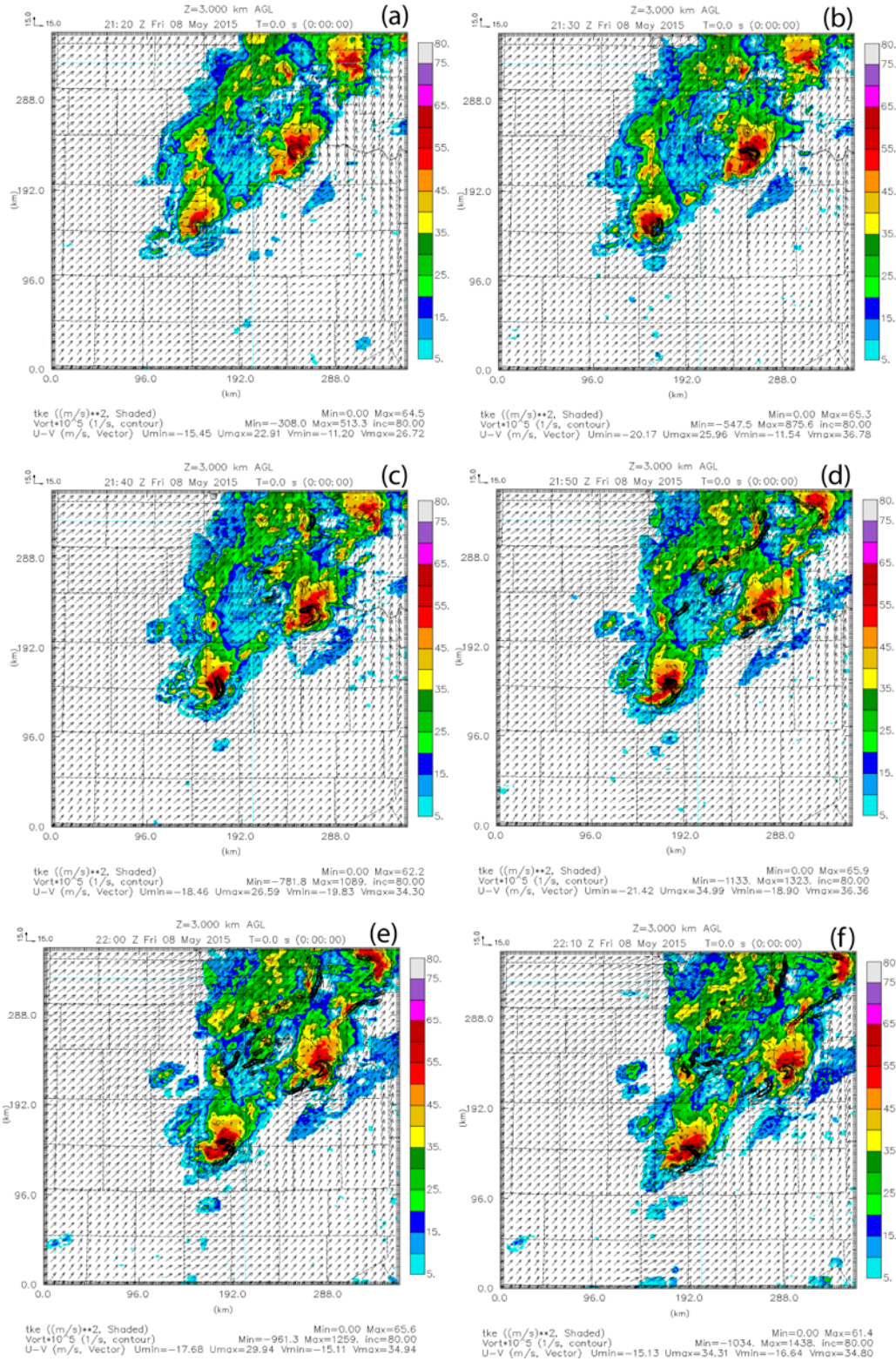


Fig. 7. The analyzed reflectivity, horizontal wind fields, and vortices at $z=3$ km using data from radars displayed in Fig. 6(b) valid at (a) 2210 UTC, (b) 2230 UTC, (c) 2250 UTC, (d) 2310 UTC, (e) 2330 UTC, and (f) 2350 UTC, June 03, 2015 near south Kansas.

